Biochemical and Biophysical Research Communications 424 (2012) 141–146

Contents lists available at SciVerse ScienceDirect

Biochemical and Biophysical Research Communications

journal homepage: www.elsevier.com/locate/ybbrc

High-definition NMR structure of PED/PEA-15 death effector domain reveals details of key polar side chain interactions

Edward C. Twomey [a], Yufeng Wei [a,b,*]

[a] Department of Chemistry and Biochemistry, Seton Hall University, South Orange, NJ 07094-2646, USA
[b] Spectroscopy Resource Center, Rockefeller University, New York, NY 10065-6399, USA

ARTICLE INFO

Article history:
Received 11 June 2012
Available online 23 June 2012

Keywords:
Protein structure
Polar interactions
Protein–protein interactions
Structure determination
Structure validation

ABSTRACT

Death effector domain (DED) proteins constitute a subfamily of the large death domain superfamily that is primarily involved in apoptosis pathways. DED structures have characteristic side chain–side chain interactions among polar residues on the protein surface, forming a network of hydrogen bonds and salt bridges. The polar interaction network is functionally important in promoting protein–protein interactions by maintaining optimal side chain orientations. We have refined the solution DED structure of the PED/PEA-15 protein, a representative member of DED subfamily, using traditional NMR restraints with the addition of residual dipolar coupling (RDC) restraints from two independent alignment media, and employed the explicit solvent refinement protocol. The newly refined DED structure of PED/PEA-15 possesses higher structural quality as indicated by WHAT IF *Z*-scores, with most significant improvement in the backbone conformation normality quality factor. This higher quality DED structure of PED/PEA-15 leads to the identification of a number of key polar side chain interactions, which are not typically observed in NMR protein structures. The elucidation of polar side chain interactions is a key step towards the understanding of protein–protein interactions involving the death domain superfamily. The NMR structures with extensive details of protein structural features are thereby termed high-definition (HD) NMR structures.

1. Introduction

Death effector domain (DED) structures, together with death domain (DD), caspase recruitment domain (CARD), and pyrin domain (PYD), constitute the death domain superfamily of structures that are predominantly involved in assembly and activation of apoptotic complexes [1]. These structural domains are similarly folded into a six-helix bundle, while their homotypic interactions distinguish various subfamilies. In addition to the domain–domain interactions, DED structures are characterized by markedly conserved surface feature of a hydrogen-bonded network among the side chains of three charged residues, D/E-RxDL (x = any residues), termed the charge triad, located on helices H2 and H6. The charge triad structural feature and other extensive hydrogen bonding interactions among polar and charged side chains on the protein surface were first observed in high resolution crystal structures of a viral FLICE-like inhibitory protein (v-FLIP), MC159, which consists of two tandem DEDs [2,3]. These side chain-side chain interactions are suggested to be functionally important by maintaining precise side chain orientations.

PED/PEA-15 (phosphoprotein enriched in diabetes/phosphoprotein enriched in astrocytes, 15 kDa) is a small, non-catalytic protein that contains a canonical DED and an irregularly structured C-terminal tail, and regulates various cellular processes, such as apoptosis, cell proliferation, and glucose metabolism [4]. Together with MC159 and FADD (fas associated death domain protein) [5] DED, PED/PEA-15 is one of the founding members that established the surface charge-triad interactions [6]. However, the current PED/PEA-15 NMR structure (PDB ID: 1N3K) [7] does not allow the identification of the charge triad and other side chain hydrogen bonding and salt bridge interactions (referred to as polar interactions) on the DED surface, due to the intrinsic limitation of conventional NMR restraints and structural refinement protocol that compromises the non-bonded and electrostatic interactions.

Over the past decade, long-range NMR restraints, such as residual dipolar couplings (RDCs) and paramagnetic relaxation enhancements (PREs), have been widely employed to supplement the traditional local restraints (chemical shifts, NOEs, dihedral angles, etc.) in obtaining NMR protein structures [8], and new protocols to refine NMR protein structures in explicit solvent have been developed to greatly improve the structural quality factors of pro-

Abbreviations: DED, death effector domain; DD, death domain; NMR, nuclear magnetic resonance; PED/PEA-15, phosphoprotein enriched in diabetes/phosphoprotein enriched in astrocytes, 15 kDa; RDC, residual dipolar coupling.

* Corresponding author. Address: Department of Chemistry and Biochemistry, Seton Hall University, 400 South Orange Ave., South Orange, NJ 07094-2694, USA. Fax: +1 973 761 9772.
E-mail address: Yufeng.Wei@shu.edu (Y. Wei).

0006-291X/$ - see front matter © 2012 Elsevier Inc. All rights reserved.
http://dx.doi.org/10.1016/j.bbrc.2012.06.091

teins [9]. In this research, we have refined the PED/PEA-15 DED NMR structure using the explicit water refinement protocol with the addition of RDC restraints measured from two independent alignment media. This newly refined DED structure allows us to evaluate the extensive surface hydrogen bonding and salt bridge interactions among the charged and polar side chains, including the charge triad, as a result of significantly improved backbone conformation normality and more realistic treatment of non-bonded and electrostatic interactions. It is of great importance to elucidate these functionally essential polar interactions, which are key to the understanding of how DED structures can mediate protein–protein interactions in a wide variety of cellular processes. We have termed these NMR structures with extensive details of side chain–side chain interactions as high-definition (HD) NMR structures.

2. Materials and methods

2.1. NMR spectroscopy

Expression of the ^{13}C,^{15}N-labeled PED/PEA-15 for NMR spectroscopy was conducted as previously described [7]. All NMR experiments were performed at 25 °C using a Bruker Avance 600 spectrometer equipped with a triple-resonance cryoprobe. The two alignment media for RDC measurements were filamentous bacteriophage pf1 with a final concentration of ~9 mg/ml [10,11], and a 5% nonionic liquid crystalline solution formed by *n*-alkyl-poly(ethylene glycol), denoted $C_{12}E_5$ (Fluka), and *n*-hexanol (Aldrich) in water, with $C_{12}E_5$/hexanol molar ratio $r = 0.85$ [12]. The ^{1}H–^{15}N RDCs were measured using spin-state selective coherence transfer (S^3CT) in-phase antiphase (IPAP) technique [13]. All NMR spectra were processed with NMRPipe [14] and analyzed using NMRViewJ [15]. Initial values for the axial component (D_a) and the rhombicity (R) of the dipolar coupling tensor were estimated from a normalized histogram of measured RDCs [16] using the analysis toolkit iDC [17].

2.2. Structure calculations

The PED/PEA-15 DED structures (residues 1–90) were calculated with the program XPLOR-NIH (version 2.29) adapted to incorporate pseudopotentials for $^{3}J_{NH\alpha}$ coupling constants, secondary $^{13}C_\alpha$ and $^{13}C_\beta$ chemical shifts, a conformational database potential for dihedral angles, and a harmonic potential for the refinement against RDCs [18,19]. All original restraints used in the calculation of the PDB file 1N3K [7], as well as ^{1}H–^{15}N RDC restraints measured from both $C_{12}E_5$/hexanol and bacteriophage pf1 media were included in current calculations. Twenty calculated structures were selected for additional refinement in explicit water solvent with PARALLHDG 5.3 force field [9]. The agreement between expected and calculated RDC values was determined by singular value decomposition (SVD) analysis [20] implemented in the iDC toolkit [17]. Structural quality was assessed with PROCHECK/PROCHECK_NMR [21] and WHAT IF (version 8) [22]. Structures were displayed and analyzed using PyMOL version 1.5 (http://www.pymol.org/) on a Linux workstation. The cutoff used for the hydrogen bonding and salt bridge interactions was 3.20 Å for the heavy atom distance.

3. Results

3.1. Structure determination

We determined the three-dimensional structure of the PED/PEA-15 death effector domain, residues 1–90, using a total of 2417 NMR restraints, including the original NMR restraints (1985 NOE distance restraints, 230 φ and ψ dihedral angle restraints from the TALOS analysis of $^{13}C_{\alpha/\beta}$ chemical shifts, and 81 $^{3}J_{NH\alpha}$ coupling constants) used to solve 1N3K PDB structure, and 121 ^{1}H–^{15}N residual dipolar coupling (RDC) restraints measured in both $C_{12}E_5$/hexanol and bacteriophage pf1 media. The 20 lowest-energy structures were further refined in explicit solvent (Fig. 1A) as previously described [23]. The protein backbone is very similar to the existing 1N3K structure with RMSD for C_α atoms of 0.526 Å (Fig. 1B). Comparing to 1N3K, our model agrees better with experimental restraints, particularly the distance (NOE) restraints, dihedral angle restraints, and $^{3}J_{NH\alpha}$ coupling constants (Table 1). Detailed inspection of the two models of PED/PEA-15 DED structures further reveals great structural features, especially the side chain–side chain interactions, in our currently refined model (see text below). The newly refined structures fit the dual-medium RDC sets simultaneously with excellent agreement between the predicted and experimental values (see Supplementary material Fig. 1).

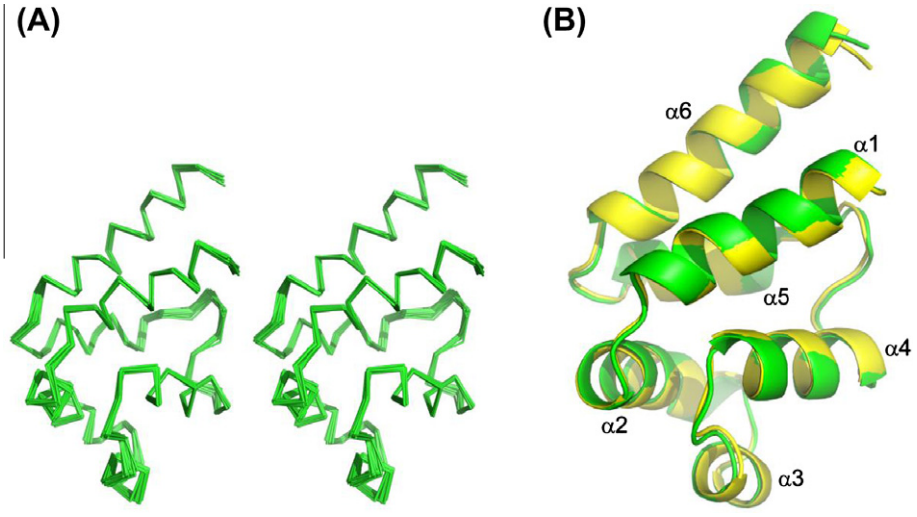

Fig. 1. Three dimensional structure of PED/PEA-15 DED. (A) Stereo superposition (cross-eyed) of the backbone atoms of for the 20 members of the PED/PEA-15 DED structure family refined with dual-medium RDC sets in explicit solvent. (B) A ribbon representation of currently refined model of PED/PEA-15 DED superimposed with previously refined 1N3K model. Only the DED (residues 1–90) of the 1N3K model is shown here. The RMSD among all Ca atoms is 0.526 Å.

Table 1
NMR and refinement statistics for PED/PEA-15 DED residues 1–90.

	1N3K*	In water
Violations (mean and s.d.)		
Distance constraints (1985) (Å)	0.067 ± 0.001	0.039 ± 0.001
Intra-residue (341)	0.071 ± 0.003	0.048 ± 0.004
Sequential ($\|i-j\|=1$) (464)	0.062 ± 0.003	0.038 ± 0.002
Medium-range ($\|i-j\|\leqslant 5$) (611)	0.072 ± 0.002	0.039 ± 0.002
Long-range ($\|i-j\|>5$) (483)	0.067 ± 0.002	0.037 ± 0.002
Hydrogen bonds (86)	0.008 ± 0.005	0.005 ± 0.004
Dihedral angle constraints (230) (°)	0.23 ± 0.06	0.20 ± 0.07
$^3J_{NH\alpha}$ coupling constants (81) (Hz)	0.80 ± 0.02	0.71 ± 0.02
Max. dihedral angle violation (°)	–	0.29
Max. distance constraint violation (Å)	–	0.041
$^1D_{NH,\ bacteriophage\ pf1}$ (58) (Hz)	–	0.51 ± 0.03
Q (%)	–	2.3
$^1D_{NH,\ C12E5/hexanol}$ (63) (Hz)	–	0.67 ± 0.04
Q (%)	–	2.6
Deviations from idealized geometry		
Bond lengths (Å)	0.0041 ± 0.0001	0.0157 ± 0.0003
Bond angles (°)	0.60 ± 0.02	2.90 ± 0.04
Impropers (°)	0.56 ± 0.02	3.64 ± 0.05
*Average pairwise r.m.s. deviation*** *(Å)*		
Backbone (2–89)	0.16 ± 0.02	0.27 ± 0.04
All heavy atoms (2–89)	0.62 ± 0.02	0.70 ± 0.04
Quality factors		
% Residues in most favorable region of Ramachandran plot	89.8	90.8

* Only data for residues 1–90 of 1N3K is tabulated.
** Pairwise r.m.s. deviation was calculated among 20 refined structures.

3.2. DED surface polar interactions

Although the PED/PEA-15 1N3K model is a well-refined structure, some key information is lacking from the model. Most significantly, the model does not delineate the charge-triad D^{19}–R^{72}xD^{74}L interactions (Fig. 2A), a key and distinct surface feature that characterizes DED subfamily proteins and distinguishes them from other DD superfamily proteins. In our refined model, we can easily identify both D^{19}–R^{72} pair and R^{72}–D^{74} pair of the charge-triad interactions in 14 out of the lowest energy 20 structures, with 11 structures containing the complete D^{19}–R^{72}–D^{74} motif. Other structures in the assemble represent the dynamic natures of the NMR structures, in which the polar side chain interactions are transiently fluctuating away from the equilibrium state. It is also noteworthy that there are no direct experimental distance or orientation restraints to define polar side chain–side chain interactions during the refinement. In addition to the charge-triad motif, a number of other side chain–side chain hydrogen bonding and electrostatic interaction pairs can be detected in our model, including highly occurring pairs D^{56}–N^{59}, D^{81}–R^{85}, and R^{83}–T^{84}, and moderately occurring pairs E^{3}–R^{85}, D^{10}–N^{13}, D^{10}–R^{85}, T^{16}–D^{19}, E^{21}–K^{24}, E^{34}–K^{35}, K^{35}–E^{38}, S^{47}–E^{50}, E^{64}–R^{83}, and H^{65}–E^{68}. A full list of interaction pairs is available in Supplementary material Table 4. Among these interaction pairs, many residues are functionally important to PED/PEA-15. For example, residues 7–17 consists of the nuclear exporting sequence (NES) that localizes PED/PEA-15 and bound ERK1/2 proteins in the cytosol [24], and T16 and D74, among a few other residues, are essential in ERK2 binding [7]; polar residues in between 1 and 24 are necessary for phospholipase D1 interaction, which ultimately leads to type II diabetes [25]. A representative model structure of refined PED/PEA-15 DED with surface polar interactions is illustrated in Fig. 2B and 2c. Based on the fact that our NMR PED/PEA-15 DED model has greater details on the polar side chain interactions, prominently similar to a crystal structure while commonly lacking from NMR structures, we have referred to our structure as "high-definition (HD) NMR structure". It is noted that "high resolution NMR structure" be avoided

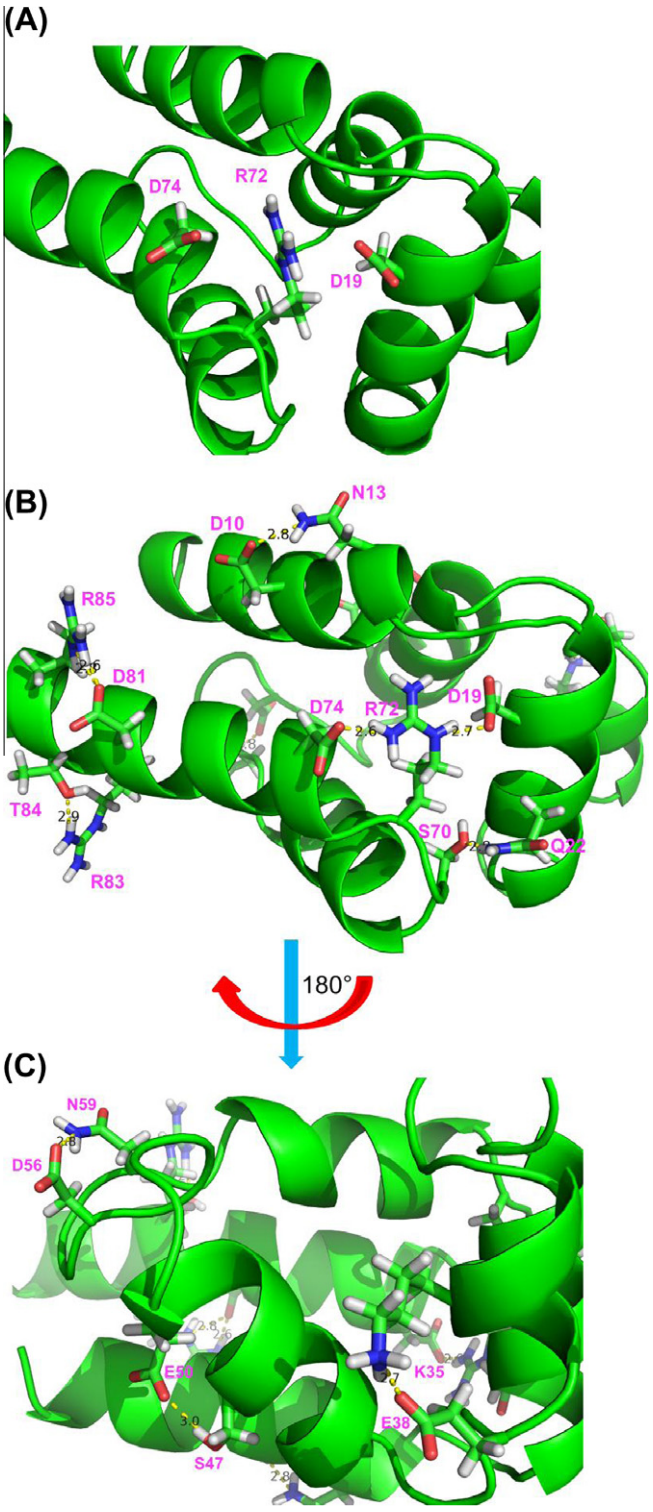

Fig. 2. Surface polar (hydrogen bonding and salt brige) interactions for the DED of PED/PEA-15 in 1N3K residues 1–90 (A) and currently refined model (B) and rotated in 180° (C). The side chains of interests are represented in sticks, and the residues are labeled in magenta. Hydrogen bonding interactions are identified by the dashed lines with distances displayed between the two heavy atoms. The side chains of the charge-triad, D^{19}–R^{72}–D^{74}, in 1N3K are not properly oriented with unsatisfied hydrogen bond donors and acceptors (A), while the side chains of the charge triad residues are oriented properly in our model, and the hydrogen bonding network is readily identified among the three residues (B). A number of additional hydrogen bonding and salt bridge interactions are also observed in our model. (For interpretation of the references to colour in this figure legend, the reader is referred to the web version of this article.)

Table 2
WHAT IF structural quality indicators for PED/PEA-15 DED residues 1–90.

	1N3K*	Current model
Structure Z-scores (positive is better than average, <−3.00 poor, <−4.00 bad)		
1st generation packing quality	0.316	−0.063
2nd generation packing quality	−1.179	−1.094
Ramachandran plot appearance	−0.274	−1.222
χ_1/χ_2 rotamer normality	−2.577	−2.840
Backbone conformation	−3.879	0.810
RMS Z-scores (should be close to 1.0)		
Bond lengths	0.309 (tight)	1.059
Bond angles	0.502 (tight)	1.061
ω Angle restraints	0.241 (tight)	0.980
Side chain planarity	0.152 (tight)	1.744
Improper dihedral distribution	0.530	1.858 (loose)
Inside/outside distribution	0.990	1.010

* All *Z*-scores are calculated for residues 1–90 only of 1N3K.

as NMR structures do not contain resolution information as in crystal structures.

3.3. Structure validation

The quality of our current model and 1N3K was vigorously accessed using structure validation programs PROCHECK/PROCHECK_NMR and WHAT IF. All reported quality indicators are evaluated using only the DED structure of PED/PEA-15, residues 1–90. In the 1N3K model, the C-terminal tails (residues 91–130) were removed from the PDB file before being validated by either program so that the irregularly structured C-terminal tail would not affect the overall or per-residue scores. The PROCHECK Ramachandran property improved slightly from 89.8% residues in most favorable region in 1N3K to 90.8% in our model. The remaining residues are all in the additionally allowed region. No residues appear in either generously allowed region or disallowed region of the Ramachandran plot for both models. The overall WHAT IF structural quality indicators (*Z*-scores) are summarized in Table 2. The structure *Z*-scores are comparable between the two models, with the exception of the backbone conformation *Z*-score which is significantly improved in our current model (0.810) comparing to 1N3K (−3.879). The RMS *Z*-scores are also improved markedly in our current model, which relaxes the intrinsically over-restrained local geometries of bond lengths, bond-angles, ω-angles, and side chain planarity in 1N3K.

The more informative per-residue structure validations [26] on both 1N3K and our model are shown in Fig. 3. The WHAT IF *Z*-scores for 1st and 2nd generation packing quality, Ramachandran plot appearance, χ_1/χ_2 rotamer normality all fall in a similar range for both models. The backbone conformation normality *Z*-score indicates significant improvements in our current model, particularly in the helices α5 and α6. Besides the loop and flexible regions, which commonly show low backbone normality scores, the regular secondary structural elements (the α-helical regions) in our structure score consistently well throughout the sequence. In the 1N3K model, however, low backbone normality scores are observed in residues 36 (α3), 43, 47 (α4), 65 (α5) and 79–82 (α6). Improved backbone normality and optimized side chain orientations allow the formation of desired polar interactions to be observed.

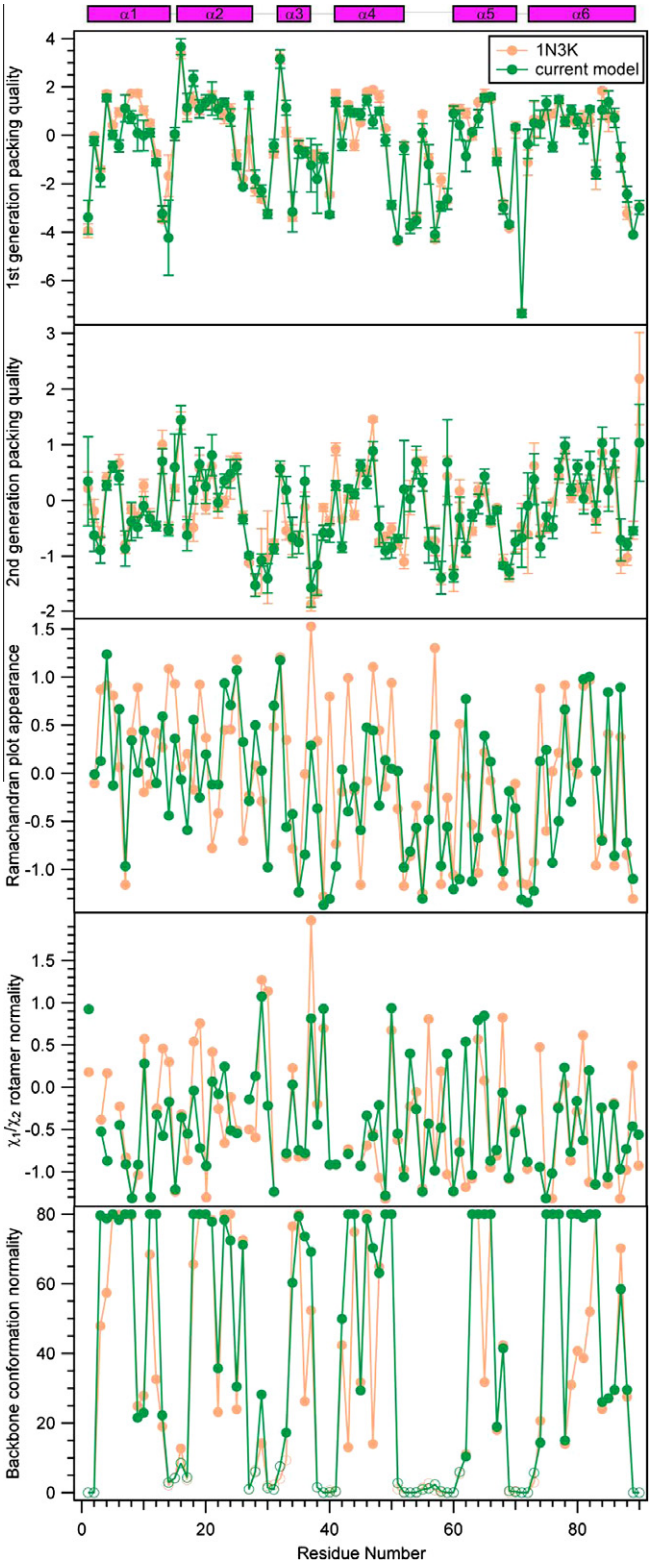

Fig. 3. Five different per-residue structural quality indicators from WHAT IF. (A) 1st generation packing quality *Z*-score. (B) 2nd generation packing quality *Z*-score. (C) Ramachandran plot appearance *Z*-score. (D) χ_1/χ_2 rotamer normality *Z*-score. (E) Backbone conformation normality *Z*-score. The values listed on the *y*-axis indicate the number of times the local backbone (defined by the current residue plus or minus two residues) was found in WHAT IF's internal database (with a cut-off on the number of hits at 80). The α-helical secondary structures are indicated on top of the plot. No statistically significant difference between the two models for the first four *Z*-scores, while the backbone normality *Z*-score shows that our current model has greatly improved backbone normality, especially in the helices α5 and α6. The *Z*-scores for 1N3K were calculated only for residues 1–90, and are used here in the comparison.

4. Discussions

In order to obtain HD NMR structures that show the key surface polar side chain interactions, in our opinion, the structure should be refined against RDCs measured from at least two orthogonal media in addition to other conventional NMR restraints, and the

explicit solvent refinement protocol should be employed. RDCs measured from slightly aligned samples provide long-range orientational restraints for individual bond vectors with respect to the external magnetic field, which is described by the molecular alignment tensor [27]. RDC data measured from two or more media is more important than multiple RDC types ($^1H–^{15}N$, $^1H_\alpha–^{13}C_\alpha$, $^{13}C'–^{15}N$, etc.) measured from a single medium. RDCs measured from a single medium provide only one molecular alignment tensor, regardless how many types of RDCs measured. The solution of the bond vector orientations from single alignment tensor is not unique. RDCs from multiple alignment media, even only one type of RDC (such as $^1H–^{15}N$) in each medium, will provide multiple orthogonal molecular alignment tensors, which will help to resolve the degeneracy of the orientations of the bond vectors. As a result, a more accurate bond vector will be obtained from multiple-medium RDC data. In our current refinement of the high-definition PED/PEA-15 DED structure, we have included $^1H–^{15}N$ RDCs from two independent media that are orthogonal to each other (see Supplementary material Fig. 2), leading to a substantial improvement in the backbone conformation normality *Z*-scores (−0.407) comparing to 1N3K (−3.879) even before explicit water refinement.

NMR NOE-based distance restraints are excellent for observing hydrophobic interactions among nonpolar aliphatic and aromatic side chains, and therefore the protein hydrophobic core is normally well-defined. However, polar and charged side chains generally have no or little experimental restraints. In addition, in order to improve the computational efficiency in NMR structure calculations, non-bonded and electrostatic interactions are often severely simplified, and the non-bonded attractions and repulsions are often crudely approximated by a simple repulsive volume exclusion term during structural calculation. Such simplification and approximation, together with lack of experimental restraints, can lead to serious artifacts and poorly defined side chain orientations, such as unsatisfied hydrogen bond donors and acceptors. The explicit water refinement protocol with PARALLHDG 5.3 force field implements a full non-bonded representation [9], including Lennard–Jones van der Waals interactions and electrostatic interactions from the OPLS force field [28], provides a more realistic description of the non-bonded and electrostatic interactions. As a result, the polar and charged side chain orientations are markedly improved and hydrogen bond donors and acceptors are satisfied. The model we refined using explicit water protocol provides much greater details on the hydrogen bonding and electrostatic interaction pairs, which are considered to be crucial for PED/PEA-15 interactions with diverse proteins with no structural or functional similarities, such as other DED proteins, ERK2 (a MAP kinase), and phospholipase D1 (PLD1).

As an initial assessment of the generalizability of HD NMR structures, we revisited another similarly refined structure, the NMR structure of FADD, residues 1–191, PDB ID 2GF5, which was solved with traditional NMR local restraints combined with two sets of $^1H–^{15}N$ RDCs measured from two alignment media, and further refined with explicit water protocol [5]. The overall quality of 2GF5 model, containing both DED and DD, improved significantly over two older models of FADD from PDB, the DED only 1A1W, residues 1–83, and the DD only 1E41, residues 89–192 (with 1E3Y the average structure), as indicated by the WHAT IF quality *Z*-scores (see Supplementary material Table 1). Inspection of the 2GF5 structure also identified extensive hydrogen bonding and salt bridge interactions among polar and charged side chains on both DED and DD (see Supplementary material Fig. 3), and these interactions are not observable in either 1A1W DED or 1E41/1E3Y DD structures. It is also noted that all polar interactions for both DED and DD are on the same side of the protein (Supplementary material Fig. 3A), while essentially no polar interactions are observed on the opposite side (Supplementary material Fig. 3B). We believe this surface feature is compatible with its function as an adapter protein between Fas and procaspase-8 in forming the death-inducing signaling complex (DISC).

In addition to promoting homotypic protein–protein interactions associated with tumor necrosis factor α (TNFα)-mediated apoptosis and proliferation, DED proteins are also reported to regulate transcription, proliferation, and migration, as well as embryonic development and homeostasis of the immune system [6]. The surface polar interactions, such as the charge triad, are thought to be critical to the wide variety of functions of DED proteins. An extensive search of available structures of DED proteins in PDB gives seven structures for three unique proteins, PED/PEA-15, FADD, and the vFLIP MC159 (see Supplementary material Table 2), and only the MC159 protein has crystal structures that allow the identification of these surface polar interactions [2,3]. Besides the interactions between the two tandem DEDs in MC159, there are no DED complex structures available. On the other hand, we have found almost 20 DD structures with many unique proteins having high-resolution crystal structures. In addition, there are a number of DD complex structures that reveal DD–DD interaction patterns [29–31]. DED structures are intrinsically more flexible than DD structures, making crystallization of DED proteins more difficult. As most studies on DED proteins rely on NMR spectroscopy, the identification of the key hydrogen bonding and electrostatic interactions among surface polar and charged side chains using NMR techniques will be essential in understanding the protein–protein interactions that regulate various cellular processes. We have demonstrated here a novel approach to obtain the HD NMR structure of PED/PEA-15 that contains rich information on the polar interaction network among polar and charged amino acid side chains. This approach can be readily extended to other DED proteins (2GF5 as an example) or proteins outside the death domain superfamily.

Accession numbers

The coordinates of the high-definition PED/PEA-15 DED structure and the NMR restraints have been deposited in the Protein Data Bank with ID 2LS7 and BioMagResBank with ID 18412.

Acknowledgments

We thank Dr. Justine Hill and Yu Wei for cloning, expression, and labeling of PED/PEA-15 protein, and Dr. Justine Hill for providing 1N3K NMR restraints. We are grateful for various funding and fellowships from Seton Hall University Research Council, the Celgene Corporation, Eric F. Ross Research Fellowship, and New Jersey Space Grant Consortium/NASA.

Appendix A. Supplementary data

Supplementary data associated with this article can be found, in the online version, at http://dx.doi.org/10.1016/j.bbrc.2012.06.091.

References

[1] H.H. Park, Y.-C. Lo, S.-C. Lin, L. Wang, J.K. Yang, H. Wu, The death domain superfamily in intracellular signaling of apoptosis and inflammation, Annual Review of Immunology 25 (2007) 561–586.
[2] J.K. Yang, L. Wang, L. Zheng, F. Wan, M. Ahmed, M.J. Lenardo, H. Wu, Crystal structure of MC159 reveals molecular mechanism of DISC assembly and FLIP inhibition, Molecular Cell 20 (2005) 939–949.
[3] F.-Y. Li, P.D. Jeffrey, J.W. Yu, Y. Shi, Crystal structure of a viral FLIP, Journal of Biological Chemistry 281 (2006) 2960–2968.
[4] F. Fiory, P. Formisano, G. Perruolo, F. Beguinot, Frontiers: PED/PEA-15, a multifunctional protein controlling cell survival and glucose metabolism, American Journal of Physiology – Endocrinology and Metabolism 297 (2009) E592–E601.

[5] P.E. Carrington, C. Sandu, Y. Wei, J.M. Hill, G. Morisawa, T. Huang, E. Gavathiotis, Y. Wei, M.H. Werner, The structure of FADD and its mode of interaction with Procaspase-8, Molecular Cell 22 (2006) 599–610.
[6] M. Valmiki, J. Ramos, Death effector domain-containing proteins, Cellular and Molecular Life Sciences 66 (2009) 814–830.
[7] J.M. Hill, H. Vaidyanathan, J.W. Ramos, M.H. Ginsberg, M.H. Werner, Recognition of ERK MAP kinase by PEA-15 reveals a common docking site within the death domain and death effector domain, EMBO Journal 21 (2002) 6494–6504.
[8] A. Bax, A. Grishaev, Weak alignment NMR: a hawk-eyed view of biomolecular structure, Current Opinion in Structural Biology 15 (2005) 563–570.
[9] J.P. Linge, M.A. Williams, C.A.E.M. Spronk, A.M.J.J. Bonvin, M. Nilges, Refinement of protein structures in explicit solvent, Proteins: Structure, Function, and Genetics 50 (2003) 496–506.
[10] M.R. Hansen, P. Hanson, A. Pardi, Filamentous bacteriophage for aligning RNA, DNA, and proteins for measurement of nuclear magnetic resonance dipolar coupling interactions, Methods in Enzymology (2000) 220–240.
[11] M.R. Hansen, L. Mueller, A. Pardi, Tunable alignment of macromolecules by filamentous phage yields dipolar coupling interactions, Nature Structural Biology 5 (1998) 1065–1074.
[12] M. Rückert, G. Otting, Alignment of biological macromolecules in novel nonionic liquid crystalline media for NMR experiments, Journal of the American Chemical Society 122 (2000) 7793–7797.
[13] M.H. Lerche, A. Meissner, F.M. Poulsen, O.W. Sorensen, Pulse sequences for measurement of one-bond N-15–H-1 coupling constants in the protein backbone, Journal of Magnetic Resonance 140 (1999) 259–263.
[14] F. Delaglio, S. Grzesiek, G.W. Vuister, G. Zhu, J. Pfeifer, A. Bax, NMRPipe: a multidimensional spectral processing system based on UNIX pipes, Journal of Biomolecular NMR 6 (1995) 277–293.
[15] B.A. Johnson, R.A. Blevins, NMR view: a computer program for the visualization and analysis of NMR data, Journal of Biomolecular NMR 4 (1994) 603–614.
[16] G.M. Clore, A.M. Gronenborn, A. Bax, A robust method for determining the magnitude of the fully asymmetric alignment tensor of oriented macromolecules in the absence of structural information, Journal of Magnetic Resonance 133 (1998) 216–221.
[17] Y. Wei, M. Werner, IDC: a comprehensive toolkit for the analysis of residual dipolar couplings for macromolecular structure determination, Journal of Biomolecular NMR 35 (2006) 17–25.
[18] C.D. Schwieters, J.J. Kuszewski, N. Tjandra, G. Marius Clore, The Xplor-NIH NMR molecular structure determination package, Journal of Magnetic Resonance 160 (2003) 65–73.
[19] C.D. Schwieters, J.J. Kuszewski, G. Marius Clore, Using Xplor-NIH for NMR molecular structure determination, Progress in Nuclear Magnetic Resonance Spectroscopy 48 (2006) 47–62.
[20] J.A. Losonczi, M. Andrec, M.W.F. Fischer, J.H. Prestegard, Order matrix analysis of residual dipolar couplings using singular value decomposition, Journal of Magnetic Resonance 138 (1999) 334–342.
[21] R.A. Laskowski, J.A.C. Rullmann, M.W. MacArthur, R. Kaptein, J.M. Thornton, AQUA and PROCHECK-NMR: programs for checking the quality of protein structures solved by NMR, Journal of Biomolecular NMR 8 (1996) 477–486.
[22] G. Vriend, WHAT IF: a molecular modeling and drug design program, Journal of Molecular Graphics 8 (1990) 52–56.
[23] C.A.E.M. Spronk, S.B. Nabuurs, A.M.J.J. Bonvin, E. Krieger, G.W. Vuister, G. Vriend, The precision of NMR structure ensembles revisited, Journal of Biomolecular NMR 25 (2003) 225–234.
[24] E. Formstecher, J.W. Ramos, M. Fauquet, D.A. Calderwood, J.-C. Hsieh, B. Canton, X.-T. Nguyen, J.-V. Barnier, J. Camonis, M.H. Ginsberg, H. Chneiweiss, PEA-15 mediates cytoplasmic sequestration of ERK MAP kinase, Developmental Cell 1 (2001) 239–250.
[25] F. Viparelli, A. Cassese, N. Doti, F. Paturzo, D. Marasco, N.A. Dathan, S.M. Monti, G. Basile, P. Ungaro, M. Sabatella, C. Miele, R. Teperino, E. Consiglio, C. Pedone, F. Beguinot, P. Formisano, M. Ruvo, Targeting of PED/PEA-15 molecular interaction with phospholipase D1 enhances insulin sensitivity in skeletal muscle cells, Journal of Biological Chemistry 283 (2008) 21769–21778.
[26] S.B. Nabuurs, C.A.E.M. Spronk, G.W. Vuister, G. Vriend, Traditional biomolecular structure determination by NMR spectroscopy allows for major errors, PLoS Computational Biology 2 (2006) e9.
[27] J.H. Prestegard, H.M. Al-Hashimi, J.R. Tolman, NMR structures of biomolecules using field oriented media and residual dipolar couplings, Quarterly Reviews of Biophysics 33 (2000) 371–424.
[28] W.L. Jorgensen, J. Tirado-Rives, The OPLS [optimized potentials for liquid simulations] potential functions for proteins, energy minimizations for crystals of cyclic peptides and crambin, Journal of the American Chemical Society 110 (1988) 1657–1666.
[29] H.H. Park, E. Logette, S. Raunser, S. Cuenin, T. Walz, J. Tschopp, H. Wu, Death domain assembly mechanism revealed by crystal structure of the oligomeric PIDDosome core complex, Cell 128 (2007) 533–546.
[30] L. Wang, J.K. Yang, V. Kabaleeswaran, A.J. Rice, A.C. Cruz, A.Y. Park, Q. Yin, E. Damko, S.B. Jang, S. Raunser, C.V. Robinson, R.M. Siegel, T. Walz, H. Wu, The Fas-FADD death domain complex structure reveals the basis of DISC assembly and disease mutations, Nature Structural & Molecular Biology 17 (2010) 1324–1329.
[31] F.L. Scott, B. Stec, C. Pop, M.K. Dobaczewska, J.J. Lee, E. Monosov, H. Robinson, G.S. Salvesen, R. Schwarzenbacher, S.J. Riedl, The Fas-FADD death domain complex structure unravels signalling by receptor clustering, Nature 457 (2009) 1019–1022.